Stereoscopy in User: VR Interaction

Błażej Zyglarski[a], Gabriela Ciesielska[2][b], Albert Łukasik[2][c] and Michał Joachimiak[3][d]
[1]Faculty of Mathematics and Computer Science, Nicolaus Copernicus University in Torun, Torun, Poland
[2]Vobacom sp. z o.o. in Torun, Torun, Poland
[3]Faculty of Physics, Astronomy and Informatics, Nicolaus Copernicus University in Torun, Torun, Poland

Keywords: Stereoscopy Reconstruction, Cloud Point 3 Reconstruction.

Abstract: Viewing experience is almost natural since the surroundings are real and only the augmented part of reality is displayed on the semi-transparent screens. We try to reconstruct stereoscopy video with use of a single smartphone camera and a depth map captured by a LIDAR sensor. We show that reconstruction is possible, but is not ready for production usage, mainly due to the limits of current smartphone LIDAR implementations.

1 INTRODUCTION

Augmented Reality is modern subject, implemented by many companies, in fields of entertainment, business and education. The most significant issue is that top Augmented Reality Devices are very expensive and despite of offering extraordinary quality, can't be used widely.

Best of AR devices offer holographic screens or provide extraordinary immersion with use of stereoscopic cameras (eg. Microsoft HoloLens). Therefore, viewing experience is almost natural since the surroundings are real and only the augmented part of reality is displayed on the semi-transparent screens. The "cheap" way is "cardboard-like" headset, which allows you to use your smartphone as a screen. However most smartphones have mono - camera module placed with no chance to achieve stereoscopic view for your eyes.

We present a method to reconstruct stereoscopic view with current LIDAR-equipped phones and discuss it.

2 AUGMENTED REALITY DEVICES

In augmented reality there are two cases of stereoscopic video for the AR space. By stereoscopic video it is meant that the different background images are correctly displayed for each eye. We can distinguish devices with physical stereoscopic view as in Microsoft HoloLens devices; physical cameras converting to stereoscopic digital view as in Pico Neo 3; And digital reconstruction of surround-dings with the usage of a smartphone with a single camera

In third case, it is necessary to consider the possible ways of 3D perception and possibly find a way to reconstruct the image, which is in the basic case limited to the display picture captured by the chosen camera and duplicate it for both eyes. 3D perception is a skill developed by the human brain from a series of inputs. The basic, but not the only one, is the stereoscopic image from both eyes (most predators have stereo vision (Yang & Zhang, 2020). In the basic solution, this is not even close to perfect 3D perception.

2.1 3D Reconstruction

Modern smartphones use multiple cameras (thus they are still too close to each other when it comes to reproducing a 3D impression) and depth sensors (LIDAR) to produce depth data of the image used then in multiple "Augmented" reality apps. Having such data stream, we succeeded to produce stereoscopy reconstruction of captured image on the reference device and check possibility of its market use. The reference device on which the algorithms were tested is the iPhone 13 Pro (Max) with a LIDAR sensor and 3 cameras, from which the depth map is created.

[a] https://orcid.org/0000-0002-1822-2467
[b] https://orcid.org/0000-0001-7320-8636
[c] https://orcid.org/0000-0001-7283-7999
[d] https://orcid.org/0000-0002-4462-2376

Zyglarski, B., Ciesielska, G., Łukasik, A. and Joachimiak, M.
Stereoscopy in User: VR Interaction.
DOI: 10.5220/0011617300003417
In *Proceedings of the 18th International Joint Conference on Computer Vision, Imaging and Computer Graphics Theory and Applications (VISIGRAPP 2023) - Volume 2: HUCAPP*, pages 137-142
ISBN: 978-989-758-634-7; ISSN: 2184-4321

Table 1: Performance comparison.

CPU Performance (Single and multi-core processor tests)		Gaming Performance (GPU performance in games and OpenCL/Vulcan)	
Snapdragon 888	86	Snapdragon 888	92
A15 Bionic	99	A15 Bionic	95

In addition, the device uses the A15 Bionic processor, which is characterized by higher performance than flagship devices from the Android market (Table 1) and has 6 graphic cores for which the above-mentioned algorithms are optimized.

3 3D RECONSTRUCTION ALGORITHMS

Our goal is to explore solutions for achieving stereoscopy vision with use of smartphone device and cardboard-type headset.

3.1 Research Steps

Research steps we have taken: 1) Development of algorithms based on the depth map allowing to create at least 2,5-dimentional stereoscopic scene; 2) Checking algorithms possible efficiency and comparing them; 3) Evaluating better algorithm against source material; 4) Testing algorithms in native implementations and performance analysis; 5) Recommendation to use the algorithm in production software.

3.2 Developed algorithms

We have prepared two algorithms, which use depth cloud. A) Full 3D reconstruction using spatial point cloud, which assumes generating a 3D space based on a live depth map and displaying it as a 3D scene - generating a view for the right and left eye based on the orientation of the camera in space; and B) 2,5D Reconstruction with cutting out layers and blending them into adjusted 2D Image, with use of appropriate parallax.

Both algorithms had potential, but only algorithm A was efficient enough (on-devi ce) to use it in test case stage, and due to that is the main subject of this article.

3.2.1 Cloud Point 3D Reconstruction Algorithm

The algorithm is based on the reconstruction of the point cloud in 3D space based on live data from the LIDAR sensor.

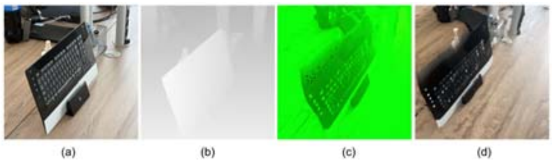

Figure 1: Steps of image analysis: (a) Texture taken from the phone camera, (b) Data from the depth sensor (LIDAR) (c) 3D scene generated on the basis of the depth sensor data (d) Scene with texture overlaid.

Reconstruction steps (as shown on Fig. 4) are: (a) texture data being acquired from the camera; (b) depth data being acquired from the LIDAR sensor; (c) construction of a 3D scene based on the depth map and filling missing parts (with resolution extrapolation); (d) Texturing of scene elements. The key stage is to complete the missing elements of the scene. The missing points are caused by the low resolution of the cloud and the shift of the point from which the virtual camera is looking (to generate a 3D view). ARKit depth mapping creates a low-resolution map. The Metal Framework has Shader (MPS) implementations that allow you to fill in the holes. In the tested case, a supplement taking the edge into account in the image analysis (MPSGuidedFilter) was used. The results are shown in Fig 2. (f) without upsampling, (a-e) with different parameters (kernel diameter - window size for algorithm (1-5), epsilon)

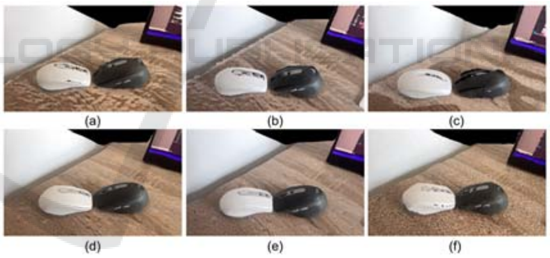

Figure 2: Using a GuidedFilter to increase the resolution of a depth map.

Guided Filter Algorithm for Resolution Upscaling

Guided Filter ("Guided filter", 2022) is a type of edge-preserving smoothing filter. It can filter out noise and texture or allow you to increase the resolution while keeping the edges sharp. Unlike the Bilateral filter ("Bilateral filter", 2022) this filter does not use calculations with linear computational complexity. The Guided Filter (Apple Developer Documentation, n.d.) can also be used to segment the image, allowing you to increase the cut quality while preserving the actual edges (Fig. 3).

Figure 3: Use of Guided Filter for edge enhancement in the image segmentation process (He, Sun & Tang, 2012).

Guided Filter is implemented natively in well-known image processing libraries, including OpenCV and iOS graphics libraries (MPSGuidedFilter).

Data Processed by the Guided Filter

The data from the depth camera, processed with the GuidedFilter algorithm, is used as the source for the 3D scene. An object is generated in the space based on the color of each pixel. Its distance from the camera is determined by the color of the pixel on the depth map.

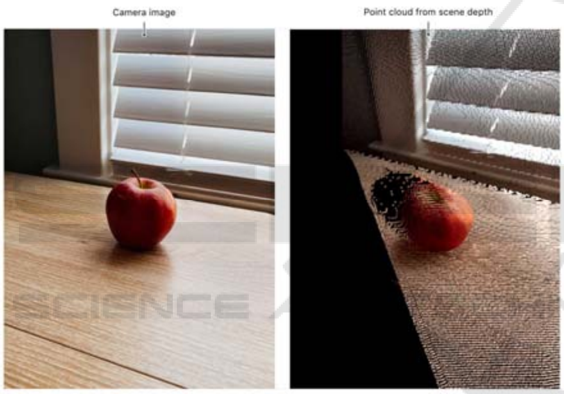

Figure 4: A 3D scene generated from the depth map, without resolution upscaling (Apple Developer Documentation, n.d.).

Scene Generation

Scene generation algorithm works as following:

1) For each point on the depth map, its position on the stage in relation to the camera (x, y) is calculated
2) Along with the depth data (color on the depth map), the position (x, y, z) is calculated where z is the distance from the camera
3) Based on the point position, the pixel color is sampled from the original image.

The scene is done using two cameras that simulate the distance between the eyes

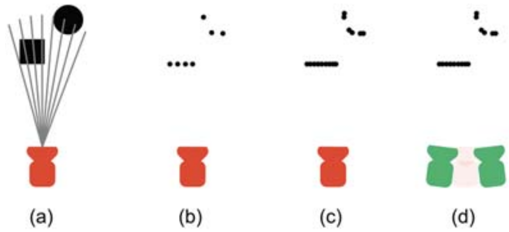

Figure 5: Rendering process (a) LIDAR depth mesh (b) detected points (c) points after processing with an algorithm increasing the resolution (d) camera viewpoints during rendering of the resulting view.

The input data from the depth sensor is quite variable. When observing a static image, we can notice differences in the consecutive collected frames (Fig 9).

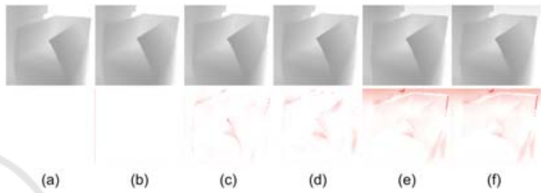

Figure 6: Differences in collected image frames.

They are especially visible at the edges. While it is not a problem in embedding objects in a 3D scene, because the ARKit/ARCore algorithms focus on surface recognition, then in the case of attempts to reconstruct the entire scene in a 3D form, they cause flickering edges. Attempting to reduce flicker by stacking the few of the last few frames (Fig 7., algorithm based on hardware image filter acceleration CoreImage) allows for greater stability with a still image but increases edge flickering during camera movement.

Figure 7: Stacking following frames.

At the same time, the readings for flat surfaces also change over time.

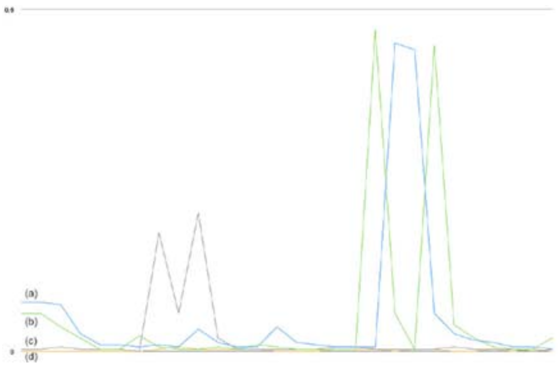

Graph 1: (a,b) High glossy surfaces flickering, (c,d) Non-glossy surfaces flickering.

Graph 1. shows examples of changes between individual frames (the average difference in the brightness of pixels on the depth map) for static views of objects with shiny surfaces (1,2) and without shiny surfaces (3,4).

Figure 8: View of an exemplary glossy surface.

The most important problem for shiny surfaces and edges is changing the pixel depth with each reading, causing the edges and shiny planes to vibrate. Part of the problem can be eliminated by averaging the frames taken from the LIDAR sensor (which, as the matter of fact, is already done by hardware preprocessing). Second problem is the lack of knowledge about pixels hidden behind edges when generating a 3D view for the other eye. The problem can be partially mitigated by the algorithms built into ARKit. However, the result is not ideal – it generates artifacts for objects located close to it, so in particular it will concern the issue of controlling and displaying controllers or hands.

Close Scene Generation Results

We developed an algorithm, which allowed us to generate scenes with few parameters toggled as "upsampling" and "stacking frames". We have displayed generated video for each eye. For better quality left eye virtual camera was placed as original camera (since original camera of the smartphone while wearing a cardboard set is nearly in front of left eye). Right eye view was generated from "virtual point of view" moved about 5 cm right (Fig 9).

Figure 9: Upsampling and edge enhancement by frames stacking.

Results were poor, especially for close objects. Averaging the pixels on the edges gives objects extra depth as the edge readings are very imprecise. Increasing the resolution of the LIDAR sensor will allow the use of a 3D image generation tool in the future. However, at this stage, the results are not satisfactory.

Inpainting Ideas

Artifacts mainly concern places where the algorithm cannot correctly calculate the distance. Tests have shown that such problems are visible on all reflective surfaces, transparent, with high detail, which is greater than the LIDAR resolution and of course we don't have enough data everywhere. In this case the best solution would be to use an inpainting algorithm filling all the gaps, but this is not the case in the "mobile" type of algorithm. All known inpainting algorithms use large datasets and are heavy loaded, unsuitable for mobile devices. Regardless of the performance results of current devices, it can be assumed that in the upcoming years more efficient smartphones will appear on the market, allowing for the use of an additional step for each layer (inpainting).

Large Scene Results

Regardless poor results in close scenes, other thing is our large and mid-range scene results, which were more than good. Example scenes are presented in Fig 10.

Figure 10: Mid-range scene.

It turns out, that missing edges data in mid- and far-range scenes can be easily simulated with Guided Filter and with big enough resolution those additions can be missed out by scene viewer.

4 ALGORITHM EVALUATION

Out of the two tested algorithms, an algorithm based on generating 3D space from a point cloud based on data collected from the LIDAR sensor was selected.

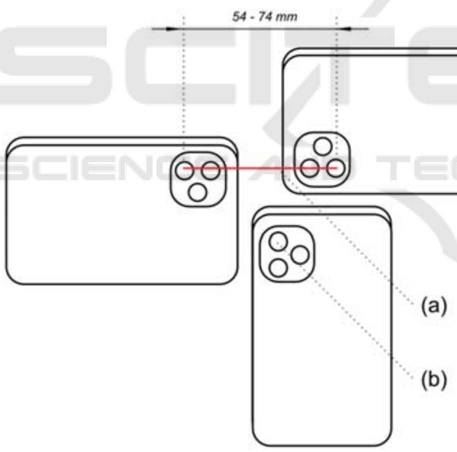

Figure 11: Device setup.

The algorithm was run on a reference device and a test video was recorded, which was later used as a survey material for the survey participants. The test material is therefore a generated stereoscopic video. The test material was compared with the reference material recorded with two identical devices to obtain a full-fledged stereoscopic video.

Test videos were recorded with three reference devices set (Fig. 11). The devices were placed on parallel stands to ensure their correct positioning. To simplify the research process, it was assumed at this stage that the reference cameras would be positioned parallel to each other, with an appropriate shift, which would allow the human eye to recognize 3D space ("Simple Stereo Camera Calibration", 2021).

4.1 Test Set

Figure 12: Regenerated stereoscopic video.

Twenty test sequences have been recorded. The test sequence consisted of a 30-second recording made with two cameras and is a full-fledged stereoscopic video or 30-second video made with one camera using 3D reproduction to generate the image of the other camera. The recordings were prepared in various test conditions, in which use seems likely due to the specificity of the solution being developed.

For example, it was desk view in medium-sized office or open space (Fig. 12).

4.2 Test Survey

Each sequence was displayed to study participants using CardBoard tools and reference smartphones. After each sequence, the user filled in the questionnaire.

The sequences were rated on a scale of 1 to 5 in the following categories each:

- On a scale of 1 to 5, determine how high you think the quality of the 3D image was
- To what scale did 3D video cause discomfort (1-small, 5-large)
- Did the 3D image feel natural?
- Was the 3D scale impression correct?
- Was the sense of distance correct?

4.3 Survey Results

Survey results was in every question better for reference real 3D stereoscopic video.

Table 3: Average survey results.

	M1	M2	M3	M4	M5	M6	M7	M8	M9	M10
Q1	3,0	2,4	4,0	2,4	3,6	2,7	4,0	3,0	3,4	2,6
Q2	2,0	3,4	1,6	2,9	1,7	2,6	1,7	2,4	1,6	2,9
Q3	3,4	2,6	4,0	2,6	4,0	2,7	3,9	3,3	4,1	2,4
Q4	3,7	3,1	4,0	3,0	4,0	2,7	4,0	3,7	3,7	3,4
Q5	3,7	3,7	4,0	3,1	3,6	3,4	4,6	4,0	4,1	3,6

It is especially visible in the quality survey question (Q1), where better quality in real video is caused by the low resolution of regenerated cloud space. All respondents stated that generated video caused some discomfort and didn't feel natural, which is also connected to low resolution. Better results were achieved in scale and distance tests, where respondents stated that impression of those was better than average. Moreover, survey results were similar in generated and real stereoscopic video.

5 CONCLUSIONS

Considering the lack of inpainting (which is a non-trivial task) and intelligent layer division (also non-trivial) in the above test, the achieved results are strongly insufficient for commercial implementation. In the case considered in this study, inpainting would have to be carried out in a quite complex range for each layer of the generated image, several dozen times per second (minimum 25, preferably around 60). This is a criterion that effectively excludes the use of this type of solution in the current state of the art. However, we recommend returning to the analysis of this task within the time frame of several years.

ACKNOWLEDGEMENTS

This paper was created as a part of the EU project "Development of a novel training ecosystem using mixed reality (MR) technology". The project is co-financed by the European Regional Development Fund under Priority Axis 1 Support for R&D by enterprises, Measure 1.1. R&D projects of enterprises, Sub-measure 1.1.1 Industrial research and development works carried out by enterprises, Intelligent Development Operational Program 2014-2020.

REFERENCES

Apple Developer Documentation. (n.d.). Retrieved October 5, 2022, from https://developer.apple.com/documentation/avfoundation/additional_data_capture/capturing_photos_with_depth

Bilateral filter. (2022). In Wikipedia. Retrieved October 5, 2022, from https://en.wikipedia.org/wiki/Bilateral_filter

Chan, T., Shen, J. (2000). Mathematical models for local deterministic inpaintings. UCLA CAM TR, 00-11.

Faugueras, O. D., Toscani, G. (1989). The calibration problem for stereoscopic vision. In Sensor devices and systems for robotics (pp. 195-213). Springer, Berlin, Heidelberg.

First Principles of Computer Vision. (2021). Simple Stereo | Camera Calibration [Video]. YouTube. Retrieved October 4, 2022, from https://www.youtube.com/watch?v=hUVyDabn1Mg

Guided filter. (2022). In Wikipedia. Retrieved October 5, 2022, from https://en.wikipedia.org/wiki/Guided_filter

Heeger, D. J., Bergen, J. R. (1995). Pyramid-based texture analysis/synthesis. In Proceedings of the 22nd annual conference on Computer graphics and interactive techniques (pp. 229-238).

He, K., Sun, J., & Tang, X. (2012). Guided image filtering. IEEE transactions on pattern analysis and machine intelligence, 35(6), 1397-1409.

Kim, J. H., Yun, Y., Kim, J., Yun, K., Cheong, W. S., & Kang, S. J. (2019). Accurate camera calibration method for multiview stereoscopic image acquisition. Journal of Broadcast Engineering, 24(6), 919-927.

Köhler, R., Schuler, C., Schölkopf, B., & Harmeling, S. (2014). Mask-specific inpainting with deep neural networks. In German conference on pattern recognition (pp. 523-534). Springer, Cham.

Raajan, N. R., Philomina, B. M. A. J., Parthiban, D., & Priya, M. V. (2012). Camera calibration for stereoscopic technique. In IEEE-International Conference on Advances in Engineering, Science And Management (ICAESM-2012) (pp. 582-585). IEEE.

Tschumperlé, D., & Deriche, R. (2005). Vector-valued image regularization with

PDEs: A common framework for different applications. IEEE transactions on pattern analysis and machine intelligence, 27(4), 506-517.

Venkatesh, M. V., Cheung, S. C. S., & Zhao, J. (2009). Efficient object-based video inpainting. Pattern Recognition Letters, 30(2), 168-179.

Yang, H., & Zhang, Z. (2020). Depth image upsampling based on guided filter with low gradient minimization. The Visual Computer, 36(7), 1411-1422.